Selective Actuation of Antisymmetric Lamb Waves Using Internal d_{15} Transducers for SHM

Hussain Altammar[1] , Parry Carrison[2],
and Nathan P. Salowitz[2(✉)]

[1] University of Jamestown, Jamestown, ND 58405, USA
[2] University of Wisconsin-Milwaukee, Milwaukee, WI 53211, USA
Salowitz@UWM.edu

Abstract. Advanced capabilities of ultrasonic SHM in thin plates, like identification of damage type and compensation for environmental effects, regularly depend on the knowledge and analysis of specific wave propagation modes. Antisymmetric wave propagation modes have been identified as being particularly useful for these purposes because of their relatively slow propagation velocity and associated short wavelength at these frequencies.

Recent studies have found that location of shear deforming (d_{15}) piezoelectric actuators and sensors at the neutral axis of a beam or plate-like structure exclusively actuate and sense antisymmetric wave propagation modes, rejecting symmetric modes.

This paper presents results from recent investigations into the properties of ultrasonic wave generation and detection using d_{15} piezoelectric transducers internally embedded within structures, including effects of transducer placement through the structure's thickness, off the neutral axis.

Experimentally validated simulations found that locating a d_{15} actuator inside a structure, but off of the neutral axis increases deflections indicative of symmetric waves but did not diminish antisymmetric deflections. While the overall trends were similar, the specific results varied with frequency. Simulations and experiments were also performed to investigate the ability of systems employing d_{15} transducers to detect bond line defects in laminate beams.

Keywords: Ultrasonic · Shear deformation · Actuator · Sensor · Transducer · d_{15} · Mode selection · Antisymmetric · Bond line damage

1 Introduction

Embedded ultrasonic inspection systems enable some of the most advanced capabilities in structural health monitoring (SHM). Detection, location, characterization, and quantification of damage is possible through detailed analysis of changes in the elastic waveforms propagated through a structure.

1.1 Background

Typical ultrasonic (SHM) systems are composed of lead zirconate titanate (PZT) piezoelectric transducers permanently mounted on a structure to actuate and sense elastic waves. It is common to use piezoelectric wafer active sensors (PWASs) employing the d_{31} piezoelectric property or interdigitated transducers (IDTs) employing the d_{33} piezoelectric property mounted on the surface or embedded within a structure [1–3]. The signals produced by these systems mounted on thin beam and plate like structures are complex and hard to interpret because of the existence and coupling to multiple Lamb wave propagation modes.

Lamb waves include symmetric modes, with in plane particle displacements in the direction of propagation that are symmetric across the midline of the plate or beam, and antisymmetric modes, with antisymmetric particle displacements across the midline of the structure [1, 4]. These different propagation modes interact differently with various forms of damage. Additionally, the different propagation modes have different propagation velocities that are dependent on the material properties, structural thickness, and frequency, and therefore are *dispersive*. As a result, signals with a spectrum of frequency content, e.g. due to modulation, distort as they propagate. At low frequency only the fundamental symmetric mode (S_0) and antisymmetric mode (A_0) can exist and the S_0 mode propagates with a higher group and phase velocities than the A_0 mode. Signals are further complicated by reflections, refractions, and mode conversions that can occur when Lamb waves interact with structural boundaries and heterogeneities. Output signals of basic SHM systems, that couple to both modes, are complicated by multiple signals overlapping, causing constructive and destructive interference. Advanced capabilities of ultrasonic SHM are dependent on analysis of the individual wave propagation modes. Additionally, analysis of the A_0 mode has been identified as being particularly useful in compensation for environmental effects [5].

Multiple approaches have been pursued to enable analysis of the various wave propagation modes including signal design, truncation of the signal, modeling, and modification of the actuators and sensors.

Hanning windows are commonly used for modulation in ultrasonic SHM because they limit the frequency bandwidth introduced while creating a time-limited signal.

Another one of the most common methods to simplify the signals produced by Lamb waves is to only look at the first wave packet arrival. This wave packet must be the fastest propagating mode traveling the shortest distance (direct path). With a long enough propagation path, discrete time signal, and differences in propagation velocities of the different modes it is simple to acquire a clean first wave packet with no other interference. At relatively low frequencies the S_0 mode propagates faster than the A_0 mode, therefore this is an effective method to identify S_0 mode. Unfortunately this method cannot acquire a clean A_0 mode when the S_0 mode exists because the A_0 mode travels slower and the information is often discarded.

Modeling of the wave propagation is also common using tools like the program DISPERSE based on the Lamb equations or finite element (FE) methods [6]. This approach is very powerful but is limited by the fact that results can only be as accurate as the input material and geometric properties. Further, if an anomaly is observed in an

experimental signal there is the inverse problem of identifying the anomaly's source using simulations, often with non-unique solutions.

Actuation and sensing techniques have also been developed to exclusively couple to specific Lamb wave propagation modes. Mode selection can be achieved by sizing or angling transducers based on the wavelength or frequency of the mode desired, known as mode tuning and wedge transducers. However, this selective coupling is only functional at one specific frequency. A pair of transducers located opposite each other on a structure can be used to identify wave modes based on in-phase (symmetric) or 180°-out-of-phase (antisymmetric) motion, unfortunately this approach requires precise placement of the transducers and cumbersome wiring to both sides of the structure. Single surface mounted devices have been developed to couple to the A_0 mode by only pressing perpendicularly against the structural surface and negating shear parallel to the surface. This has been achieved by introducing a lubricant [7] or a selectively transmitting porous silicon carbide interlayer [5] between the transducer and structure. Unfortunately this results in weak transduction (actuating against the transducer's mass or an added mass and lost energy) and potential introduction of a contaminant.

Recent research has found that integration of a shear deforming PZT transducer, employing the d_{15} piezoelectric property, located at the neutral axis of a beam or plate like structure exclusively couples to antisymmetric waveforms for both actuation and sensing purposes [3, 8–15].

This paper presents the results of recent research into the effect of off neutral axis location of the transducer on mode selectivity to identify optimal transducer placement followed by a study of inspection of a laminate beam using d_{15} PZTs undergoing 3-point bending to introduce bond line damage.

2   Approach

A combination of finite element modeling and experimental tests were performed to inspect the strain and electrical signals produced by d_{15} transducers embedded within plate and beam like structures. Matching FE models and experimental specimens were created and results compared to validate the model. Then, a parametric study was performed using FE to evaluate the effects of moving the d_{15} actuator through the thickness of the structure on the mode selectivity. Finally, a laminate beam specimen with an internally embedded d_{15} PZT actuator and sensor, in a pitch-catch configuration, was subjected to a 3 point bending test to introduce bondline damage and inspected using the d_{15} PZTs. An additional d_{31} PWAS was mounted on the surface of the specimen adjacent to the sensing d_{15} PZT to enable signal comparison.

3   Methods

Experimental beam specimens were created composed of two layers of 1 mm thick 6061-T6 Aluminum. Shear deforming d_{15} PZT transducers composed of APC-850 were placed between the aluminum sheets with appropriate wiring, attached with CircuitWorks 2400 conductive epoxy [16], oriented so that the polarization <3>

directions of the PZTs were co-linear in the global <X> direction and the electrodes <1> aligned with the global <Z> direction, as shown in Fig. 1 [2]. Finally the aluminum sheets were bonded together with the PZTs between them using Loctite EA 9394 epoxy [17]. Because the PZTs were 1 mm thick, this resulted in a 1 mm $\pm$ 0.2 mm thick bond-line (confirmed by measurement with calipers) [14]. This resulted in a highly symmetric structure with the d-$_{15}$ PZTs located at the mid-plane neutral axis. Similar FE models were created in ANSYS using multiphysics elements to represent the PZTs, published material properties [2, 17, 18], and the idealized geometry, neglecting wiring and adhesive between the transducers and aluminum. The FE models simulated from electrical input to the actuator to electrical output from the sensor.
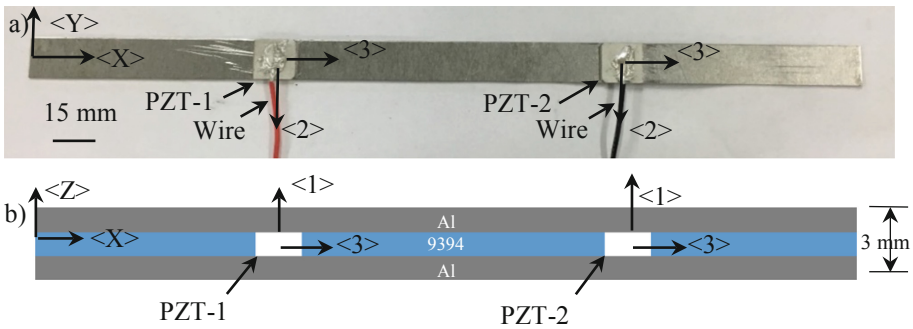

Fig. 1. Geometry of a 6061-T6 aluminum beam. a) Picture of the top of the beam with d$_{15}$ PZTs bonded in place. b) Graphic of the complete beam cross-section (side view). Local (PZT), and global coordinate systems are shown.

3.1 Model Validation

2D simulations were performed because the PZTs spanned the full beam so there was no geometric variation in the width <Y> direction as shown in Fig. 1. Simulations were also performed using DISPERSE to calculate the propagation velocities of the various Lamb wave modes, producing the dispersion curves shown in Fig. 2 [6]. Experiments and models of the pristine structure were actuated with 5-peak Hann windowed tone bursts at various frequencies and showed negligible difference between experimental signal and simulation output validating the simulation.

Simulation results were closely inspected to understand the wave propagation. The time of flight of the signals observed in both experimental data and FE simulation closely matched to the A$_0$ propagation velocity calculated with DISPERSE. Further, the <X> displacement profile shown in Fig. 3 was observed to be purely antisymmetric across the midline of the structure supporting the conclusion that actuation exclusively produced antisymmetric waves.
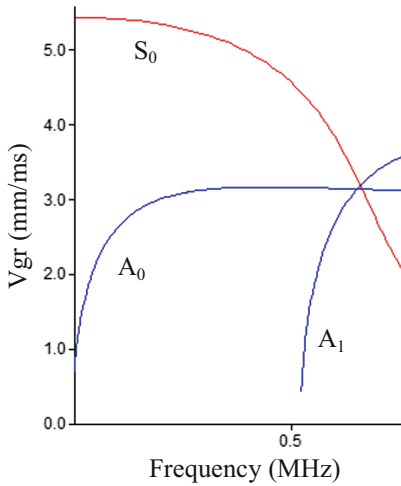
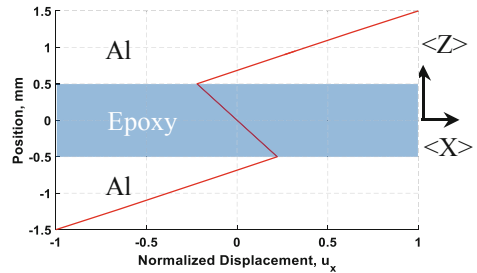**Fig. 2.** Group velocity dispersion curves for the aluminum Epoxy structure calculated in DISPERSE [6].

Fig. 3. Typical <X> displacement profile along the propagation path from the PZT-1 actuator to PZT-2sensor observed in both plate and beam simulations [3]. [14]

3.2   Parametric Study of Actuator Location Effect on Mode-Selectivity

A series of FE simulations were performed using ANSYS based on the validated model where the d_{15} actuator was moved off of the neutral axis to inspect if or how an offset would affect exclusive coupling to the A_0 Lamb wave mode. While the simulation was based on the validated work, the epoxy was replaced with aluminum properties to circumvent issues with a-symmetries due to a bondline being off the neutral axis. Simulations were performed at multiple offsets and actuation frequencies.

3.3   Damage Detection During a Three-Point Bending Test

A three-point bending test was performed with symmetric cylindrical supports 50 mm apart, a cylindrical loading head, and the structure centered in the fixture. Testing was performed with an Instron 3360 Series Universal testing system [19]. Data was acquired in a no-load condition after successively increased applied deflections. Each cycle involved subjecting the specimen to a mid-point deflection 0.1 mm greater than the prior cycle, then releasing it, and actuating d_{15} PZT-1 with a ±100 V Hann windowed 5-peak tone burst centered at 30 kHz using a KEYSIGHT 33500B Series Waveform Generator amplified through a Krohn-Hite 7602 M Wideband Amplifier [20, 21]. Signals were recorded with a Tektronix MDO3014 Mixed Domain Oscilloscope connected to the actuation channel, output of d_{15} PZT-2, and output of an auxiliary d_{31} PWAS 6 mm in diameter and 0.25 mm thick mounted on the surface adjacent to PZT-2 for comparison [22].

4   Results and Discussion

This section presents the results from each step of the work performed.

4.1   Model Validation

As previously reported, results from experimental data, FE simulation, and modeling with DISPERSE produced very similar results within 8% of the experimental result as shown in Table 1. Variation was attributed to idealization of material properties and geometry. This demonstrated that the model results and experimental results were reasonably aligned.

Table 1. Time of flight and group velocity of first arrivals [3]

	Time of flight (μs)	Group velocity (m/s)
Experiment	110.1	1181
Finite element	119.2	1090
DISPERSE S_0	-NA-	4862
DISPERSE A_0	-NA-	1154

4.2   Parametric Study of Actuator Location Effect on Mode Selectivity

Simulations were performed multiple times, actuating with Hann windowed 5-peak tone bursts at a variety of center frequencies, and with the actuator placed at, and various distances offset from the neutral axis of the beam. The maximum <X> and <Z> displacements observed along the entire neutral axis in the direct propagation were recorded and compared with <X> displacement indicating symmetric modes and <Z> displacement indicating antisymmetric modes.

As can be seen in Fig. 4a and b, when the transducer is located at the neutral axis, 0 offset, there was negligible <X> motion and significant <Y> motion at all frequencies inspected indicating negligible symmetric motion and strong antisymmetric motion. Frequency had nominal effects on the magnitude of symmetric motion, but strong effects on the antisymmetric motion. Conversely, increasing offset introduced significant symmetric motion, but had negligible effects on antisymmetric motion.
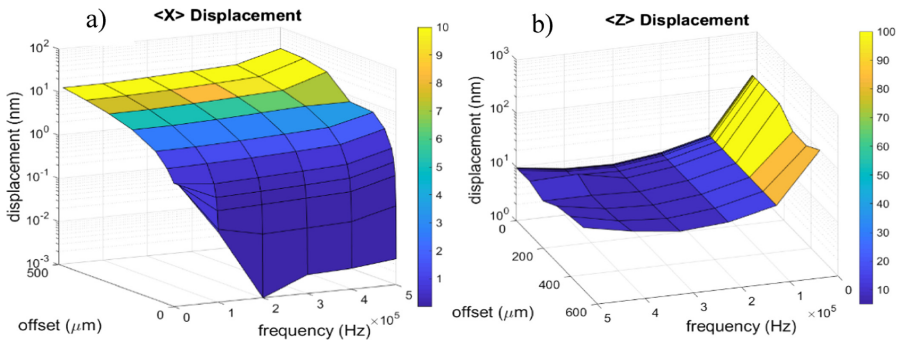
Fig. 4. Maximum displacement of particles on the neutral axis in the <X> direction (a) and <Z> direction (b) as a function of transducer position relative to the neutral axis and frequency [3].

Combined this demonstrated that offsetting the d_{15} actuator away from the neutral axis did not have a significant effect on the strength of antisymmetric waves generated, though frequency did effect the strength. However, offsetting the actuator did introduce symmetric waveforms, reducing the mode purity of the system. Therefore, to couple exclusively to antisymmetric modes, a d_{15} transducer must be located at the neutral axis. This matches theory coupling transverse shear to bending in beams and plates to bending [23–28].

4.3   Damage Detection During a Three-Point Bending Test

A three point bending test was performed on a specimen with d_{15} PZTs at the optimal location for actuating, and sensing, at the neutral axis (based on the parametric study and reversal theory) in a pitch catch configuration with an additional d_{31} sensor for comparison. The specimen was loaded to a predetermined deflection, unloaded and tested, and then deformed again to a 0.1 mm greater deflection. 33 cycles were performed with a final mid-point deflection of 3.3 mm.

Damage was first observed at the 1.0 mm deflection cycle as shown in Fig. 5a. This damage occurred at roughly the loading point and consisted of cracks in the epoxy bond line at roughly a 45° angle to the plane of the beam. Damage initiation was also observed by a drop in beam stiffness, observed in the measured load deflection curve at 1.0 mm deflection. As deflections were continually increased, damage grew to include cohesive failure near and parallel to the epoxy-aluminum interface as shown in Fig. 5b at 3.3 mm deflection.
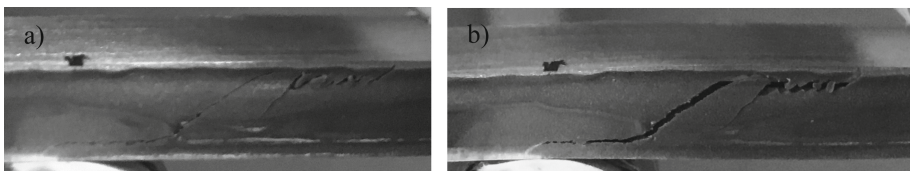

Fig. 5. Damage growth in the epoxy layer of a laminate beam subjected to three-point bending. 1) initial observed damage at 1.0 mm deflection. b) fully developed damage at 3.3 mm deflection [13]

As can be seen in the data shown in Fig. 6, the d_{15} sensor showed a greater change in signal strength than the d_{31} sensor, especially for the 3.3 mm deflection. This was also evident in the calculation of damage indices. The Pearson correlation coefficient (PCC) and normalized signal energy (NSE) were calculated based on the data [13]. The PCC showed an interesting trend with both sets of data in that it peaked at the first damage, at 1.0 mm deflection, reduced to 2.3 mm deflection, and then rose again. However, both damage indices were generally larger for the d_{15} to d_{15} combination than for the d_{15} to d_{31} system.
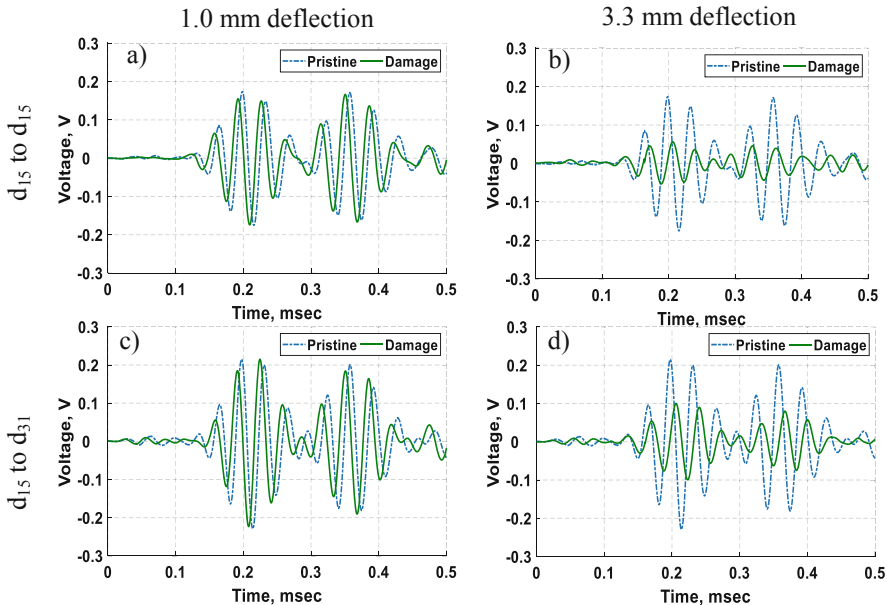

Fig. 6. Raw signals from d_{15} (a & b) and d_{31} (c & d) sensors at 1.0 mm (a & c) and 3.3 mm (b & d) displacements [13]

5   Conclusions and Future Work

A series of simulations and experiments were performed that demonstrated that use of d_{15} actuators and sensors located at the neutral axis of a beam would exclusively produce antisymmetric Lamb waves. A parametric study was performed using an experimentally validated FE model that indicated that positioning the actuator off the neutral axis would not diminish the strength of antisymmetric waves but would introduce symmetric waves, diminishing mode purity. The simulation results were independent of frequency. Finally a 3 point bending test was performed that compared the ability to detect bondline damage using a d_{15} PZT actuator at the neutral axis of a beam, and comparing the outputs of a d_{15} PZT sensor at the neutral axis to that of a d_{31} PZT located on the structural surface. It was found that the changes in the output signal

were generally greater for the d_{15} shear deforming PZT sensor, confirmed by calculation of PCC and NSE damage indices.

Future work to further understand the benefits and limitations of SHM systems based on d_{15} shear deforming PZTs include; 1) An investigation into signal strengths in both the forms of strain and voltage output relative to d_{31} PWAS based systems and 2) investigation into the effects of thinning d_{15} shear deforming transducers to reduce parasitic effects on host structures.

References

1. Giurgiutiu, V.: Structural Health Monitoring with Piezoelectric Wafer Active Sensors, 2nd edn. Elsevier, Boston (2014)
2. APC International Ltd. Physical and piezoelectric properties of APC materials, July 2020. https://www.americanpiezo.com/apc-materials/physical-piezoelectric-properties.html
3. Carrison, P., Altammar, H., Salowitz, N.: Selective actuation and sensing of antisymmetric ultrasonic waves using shear-deforming piezoelectric transducers. Struct. Health Monit. (2020) (Accepted)
4. Lamb, H.: On waves in an elastic plate. Proc. Roy. Soc. Lond. Ser. A Contain. Papers Math. Phys. Charact. **93**, 114–128 (1917)
5. Clarke, T., Simonetti, F., Rohklin, S., Cawley, P.: Development of a low-frequency high purity A0 mode transducer for shm applications. IEEE Trans. Ultrason. Ferroelectr. Freq. Control **56**(7), 1457–1468 (2009)
6. Imperial College London. Non-Destructive Evaluation: Products and Services: Disperse (2016). http://www.imperial.ac.uk/non-destructive-evaluation/products-and-services/disperse/
7. Ning, H., Shimomukai, T., Fukunaga, H., Zhongqing, S.: Damage identification of metallic structures using A0 mode of lamb waves. Struct. Health Monit. **7**(3), 271–285 (2008)
8. Altammar, H., Dhingra, A., Salowitz, N.: Ultrasonic sensing and actuation in laminate structures using bondline-embedded d35 piezoelectric sensors. Sensors **18**(11) (2018)
9. Altammar, H., Salowitz, N.: Shear actuation of piezoelectric transducers embedded within laminate structures for damage detection. In: Proceedings of the 7th Asia Pacific Workshop on Structural Health Monitoring, Hong Kong SAR, P.R. China (2018)
10. Altammar, H., Salowitz, N.: Ultrasonic inspection of bonded metal laminates using internal shear-mode piezoelectric transducers. In: Proceedings of the European Workshop on Structural Health Monitoring, Manchester, England (2018)
11. Altammar, H.: Structural health monitoring of laminate structures using shear-mode piezoelectric sensors, Ph.D. thesis ed. Milwaukee, Wisconsin, U.S.A.: University of Wisconsin - Milwaukee (2019)
12. Altammar, H., Salowitz, N.: Selective actuation and sensing of antisymmetric waves using shear-mode piezoelectric transducers. In: Structural Health Monitoring 2019, Stanford, CA (2019)
13. Altammar, H., Dhingra, A., Salowitz, N.: Damage detection using d15 Piezoelectric sensors in a laminate beam undergoing three-point bending. Actuators **8**(70) (2019)
14. Altammar, H., Dhingra, A., Salowitz, N.: Initial study of internally embedded shear-mode piezoelectric transducers for the detection of joint defects in laminate structures. J. Intell. Mater. Syst. Struct. **30**(15) (2019)

15. Altammar, H., Dhingra, A., Salowitz, N.: Investigating the feasibility of ultrasonic shear actuation for evaluation of adhesive joints in multilayered structures: FE simulation. In: American Society of Nondestructive Testing Annual Conference 2017, Nashville, TN (2017)
16. AllSpec Industries, "CW2400 - CircuitWorks Conductive Epoxy," WILMINGTON, NC, Datasheet (2012)
17. Corporation, H.: LOCTITE EA 9394 AERO Data Sheet. Rocky Hill, Connecticut (2014)
18. U.S. Department of Defense, "METALLIC MATERIALS AND ELEMENTS FOR AEROSPACE VEHICEL STRUCTURES," (2003)
19. Instron. 3360 Series Universal Testing Systems, June 2020. https://www.instron.us/products/testing-systems/universal-testing-systems/electromechanical/3300/3360-dual-column
20. Keysight Technologies, "33500B Serise Waveform Generators," Data Sheet (2017)
21. Krohn-Hite, "Model 7600 M/7602 M Wideband Power Amplifiers," Data Sheet (2018)
22. Tektronix, MDO 3000 Series Mixed Domain Oscilloscopes User Manual (2016)
23. Budynas, R.G., Nisbett, J.K.: Shigley's Mechanical Engineering Design. McGraw Hill, New York (2015)
24. Benjeddou, A., Deü, J.F.: Piezoelectric transverse shear actuation and sensing of plates, part 1: a three-dimensional mixed state space formulation. J. Intell. Mater. Syst. Struct. **12**(7), 435–449 (2001)
25. Benjeddou, A., Trindade, M.A., Ohayon, R.: A unified beam finite element model for extension and shear piezoelectric mechanisms. J. Intell. Mater. Syst. Struct. **8**(12), 1012–1025 (1997)
26. Benjeddou, A., Trindade, M.A., Ohayon, R.: New shear actuated smart structure beam finite element. AIAA J. **37**(3), 378–383 (1999)
27. Benjeddou, A., Trindade, M.A., Ohayon, R.: Piezoelectric actuation mechanisms for intelligent sandwich structures. Smart Mater. Struct. **9**, 328–335 (2000)
28. Benjeddou, A.: Shear-mode piezoceramic advanced materials and structures: a state of the art. Mech. Adv. Mater. Struct. **14**, 263–275 (2007)
29. Leo, D.J.: Engineering Analysis of Smart Materials Systems. Wiley, Hoboken (2007)